The 1993 south equatorial belt revival and other features in the Jovian atmosphere: an observational perspective

F. Moreno[1], A. Molina[1,2], and J.L. Ortiz[1]

[1] Instituto de Astrofísica de Andalucía, CSIC, PO Box 3004, E-18080 Granada, Spain
[2] Departamento de Física Aplicada, Universidad de Granada, Spain

Abstract. An excellent-quality set of images of the 1993 Jovian South Equatorial Belt (SEB) revival are shown and discussed. For the first time, this major SEB event was recorded since the very early stages of its development to its end at a variety of wavelengths from the ultraviolet to the near-infrared region of the spectrum. Our analysis supports, at least for the locus B, the Reese theory of the presence of three sources uniformly rotating with respect to System III from which the SEB disturbances develop. Other Jovian features were also present in these images, such as the activity in the South Temperate Belt or the presence of the so-called methane spots, which are shown to be photometrically analogous to the Great Red Spot on Jupiter. A general characterization of all the Jovian regions at the time of the South Equatorial Belt disturbance is done by computing the limb darkening coefficients as a function of latitude and wavelength. This provides a useful reference to compare with other future measurements. The limb darkening coefficient at the brightest spot associated to the SEB event in April shows a different behaviour in its wavelength dependence as compared to all the other Jovian regions, a result that would imply a different particle loading and/or particle size distribution in those regions as a consequence of vigorous dynamics.

Key words: planets and satellites: individual: Jupiter

1. Introduction

As early described by Peek (1958), who reported various SEB events starting in 1919-20, the outbursts of activity in the SEB are a unique event in the planet for their cataclysmic origin and development. In the present event, after a quiescent period of about three years in which the SEB showed an unusual zone-like appearance, a SEB revival occurred in April 1993. This was a major SEB disturbance after the one that occurred in 1975.

This time, the outburst was coincident with a period of coordinated observational effort by the International Jupiter Watch, within the framework of the project "World Astronomy Days #2: Jupiter atmospheric reference" (Moreno, 1993), and many results on the subject were shown at the 1993 Division for Planetary Sciences Meeting of the American Astronomical Society (see e.g. Chanover et al. 1993; Molina et al., 1993; Moreno 1993; Orton et al., 1993; Sanchez-Lavega et al., 1993). As reviewed by Reese (1972), these classical outbursts of activity tend to recur after intervals of three years or multiple of three years, although this periodicity does not always occur. The 1993 SEB revival started in April and, in August, the SEB had almost returned to its usual dark aspect in the visible. As derived from Reese's analysis, the places of the outburst seem to be linked to three permanent loci at zenographic latitude -14° that move uniformly with respect to System III longitude. The 1993 disturbance was reported to start on April 6th, 1993 with the apparition of a white bright spot at 15.5°S latitude followed by a dark column (Sanchez-Lavega et al., 1996) that sheared apart in the wind field pattern. The location of the outburst was near the locus B site as predicted by Reese (1972). In this paper, we present our first results on the observations of the onset and development of the SEB disturbance. Other interesting phenomena, such as the revival of the South Temperate Belt in various dark sectors, eruptions in the North Equatorial Belt, and the emergence of Little Red Spots at the South Tropical Zone were also recorded. The rapidly evolving dynamical activity pattern was recorded using very high resolution and high signal-to-noise ratio CCD imagery with selected narrow-band filters from the ultraviolet to near-infrared wavelengths. The good sky conditions contributed greatly to the acquisition of images of very high quality.

2. Observations

The observations were carried out at the Spanish 1.5 m telescope at Calar Alto Observatory and at the 2.5 m Nordic Optical Telescope at the Roque de los Muchachos Observatory in La Palma. Several observational campaigns covering different stages of the disturbance were conducted. Table 1 details the instrumen-
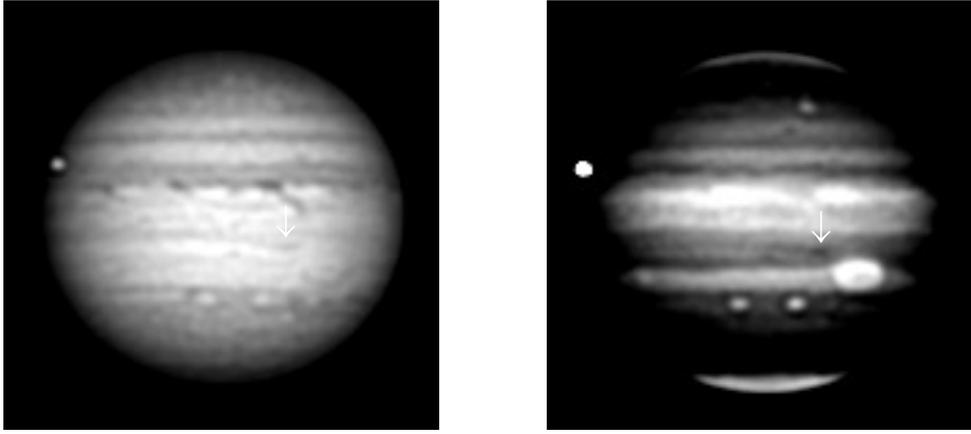
Fig. 1. Images of Jupiter through narrow-band filters at 7500 (left panel) and 8920 Å (right panel) showing a dark streak following the Great Red Spot at the same location where the South Equatorial Belt Disturbance started. These images were obtained on March 11, 1993.
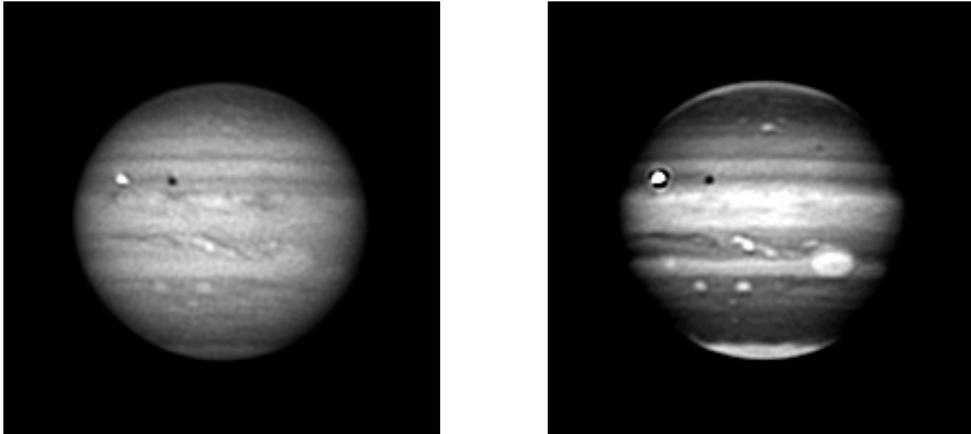

Fig. 2. Images of Jupiter showing the early stages of the SEB revival as seen in the continuum at 7500 Å(left panel) and the strong methane band at 8920 Å(right panel) on April 19, 1993.

Table 1. Log of the observations

Date (1993)	Telescope	λ range(nm)[3]	Calibrator
Mar 10-12	CAST[1]	370, 619-950	HD 111631
Apr 16-19	CAST	619-950	θ Vir
Apr 30-May 1	NOT[2]	619-950	–
May 13-14	NOT	450-950	–
Jun 2-5	CAST	370-950	η Vir[4]
			16CygB
Aug 10-12	CAST	450-950	–

[1] CAST stands for the 1.52-m Calar Alto Spanish Telescope. The CCD was a 1024×1024 UV-coated with 0.3203 arcsec·pixel^{-1}.
[2] NOT stands for the 2.5-m Nordic Optical Telescope at La Palma. The CCD was a 512×512 UV-coated with 0.1965 arcsec·pixel^{-1}.
[3] The filters are centered at 370(15), 450(10), 543(10), 619(2), 635(5), 727(2), 750(5), 892(5), 950(5) nm. Numbers between brackets indicate full width at half maximum of the filters in nm.
[4] This star was just 3.5 arcmin away from Jupiter at this date and was recorded simultaneously with Jupiter in the frames.

tation, filters and detectors used as well as the dates of the observations. The filters whose effective wavelengths are 6190 Å, 7250 Å, and 8920 Å correspond to weak, moderate, and strong methane absorption bands, respectively, in the Jovian spectrum.

All the other filters correspond to the continuum. Standard techniques for the data reduction were employed, and a Bayesian deconvolution procedure (Molina et al., 1992) was applied. The point-spread function was estimated from the Galilean satellites that were recorded simultaneously with Jupiter in the frames. Several standard stars were also used for calibration purposes as shown in Table 1.

3. The south equatorial belt revival in 1993

Briefly, this major SEB revival can be summarized as follows. Prior to the apparition of the dark column and white spot preceding it, there was a streak north preceding the GRS as recorded in our images of 10-11 March, 1993. The streak was dark at all wavelengths, suggesting a deep interior origin of this feature. After the apparition of the dark column, dark and white spots emerged from the site of the disturbance and moved with different velocities. A classical major SEB revival shows disturbances in the SEBn, "northern branch", and SEBs, "southern branch". The white spots and dark material move in opposite directions in each of the regions mentioned, and they encircle the planet in two months or less. Also, a central branch is present in a typical SEB revival. In spite of the difficulty to keep track of most features due to the continuous appearance of rapidly
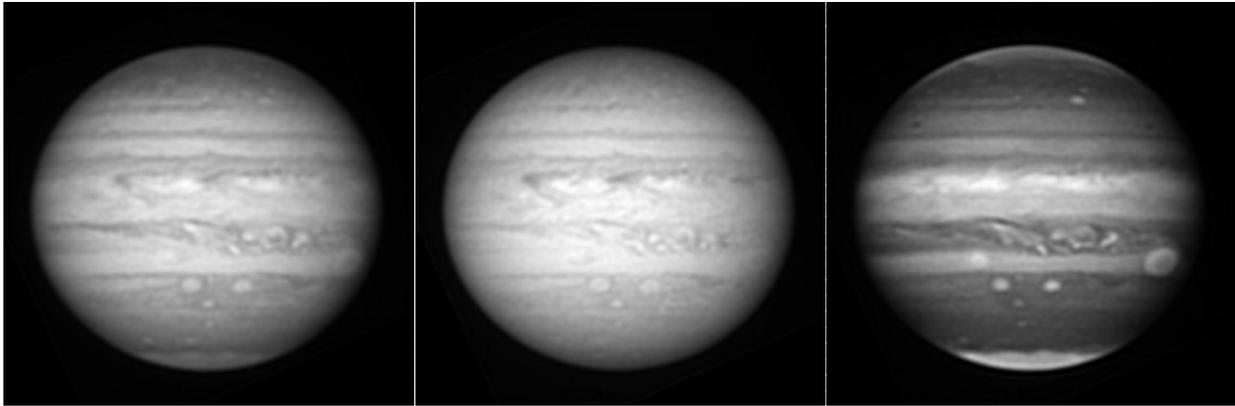
Fig. 3. Active phase of the SEB Revival as seen through different narrow-band filters (from left to right they correspond to 7250 Å, 7500 Å, and 8920 Å, respectively). The image resolution, after deconvolution, is about 0.2 arcsec. These images were obtained on April 30, 1993.
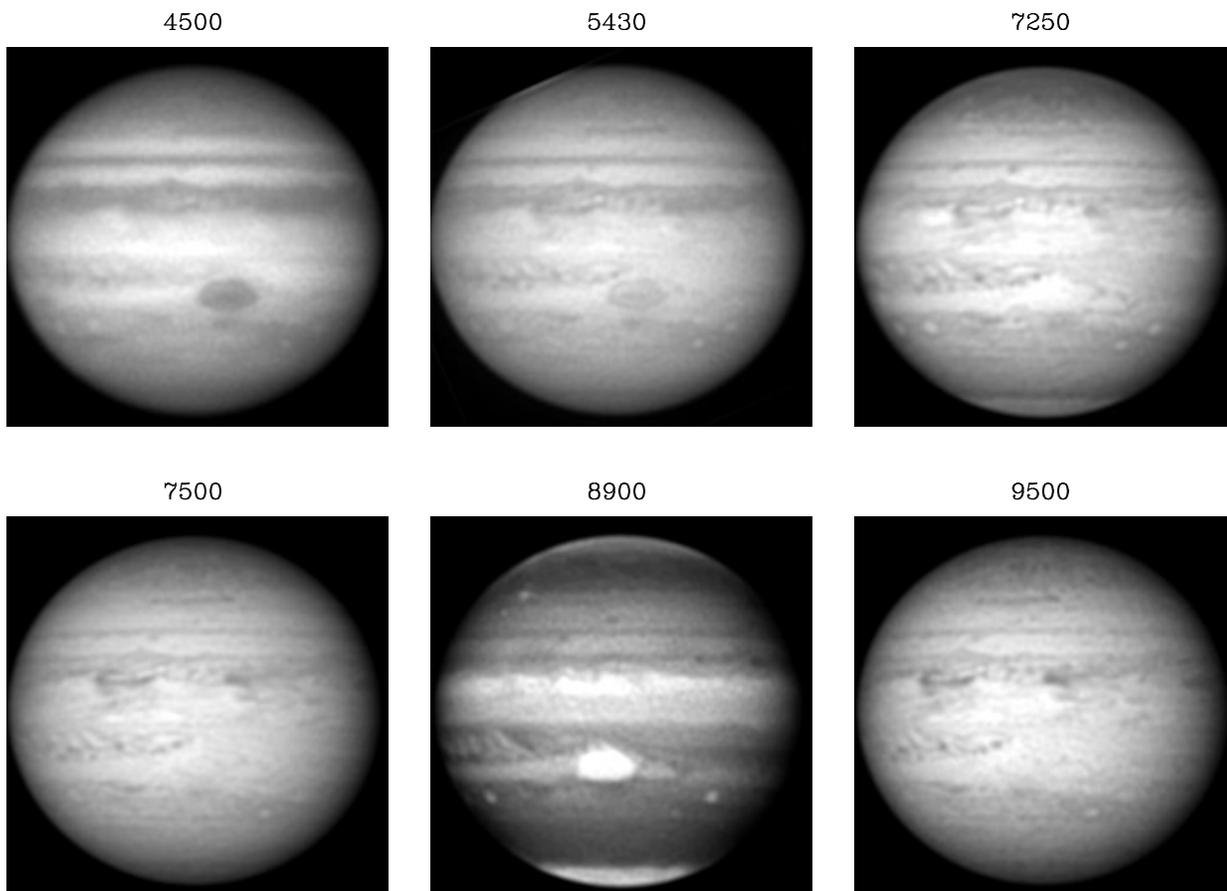

Fig. 4. Image set from 4500 to 9500 Å obtained on May 13th, 1993, showing the loss of conspicuousness of the GRS in the continuum red wavelengths (7500 and 9500 Å).
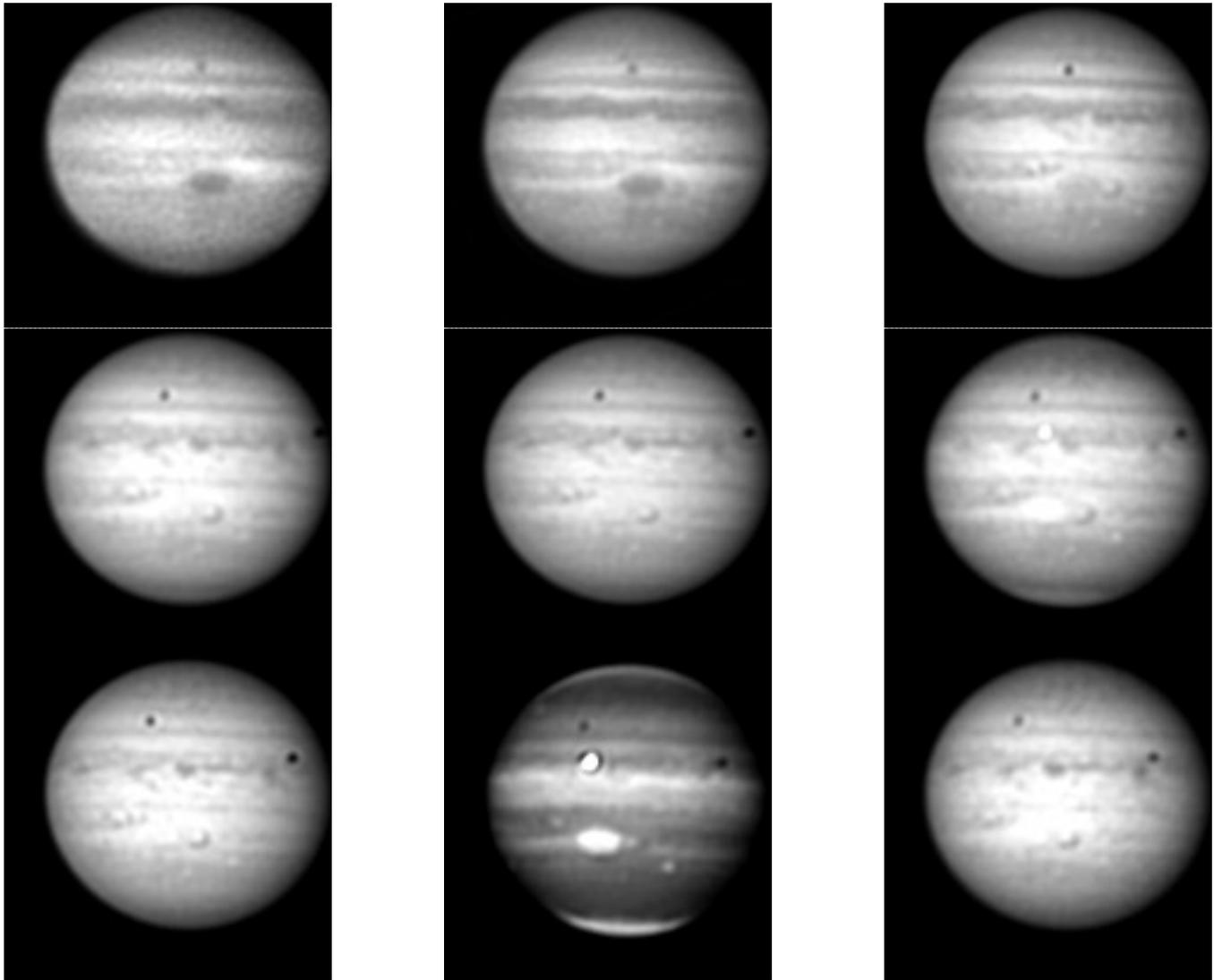
Fig. 5. Images obtained on June 3, corresponding to the wavelengths of (from left to right and top to bottom) 3700, 4500, 5430, 6190, 6350, 7250, 7500, 8900 and 9500 Å.

moving spots (Chapman and Reese, 1968) values of -5°day^{-1} for the dark material of northern branch and about -2 °day^{-1} for the central branch have been found. A southern branch of retrograding dark spots has not appeared in the 1993 SEB revival. All of these results are in good agreement with those reported by Rogers (1993). Fig. 1 and Fig. 2 show the early stages of the disturbance in March and April, 1993, as viewed through different narrow-band interference filters. Some of the white spots interacted with the GRS flow pattern, as shown clearly in the 8920Å image in Fig. 2. Just some 20 days later, the revival entered in its more active phase, as recorded in the superb images on April 30 shown in Fig. 3. The images recorded on May 13 and 14 (Fig. 4) reveal a total loss of conspicuousness of the GRS in the continuum filters (just the GRS hollow is seen), as well as some changes in its usual oval shape in the 3700, 4500 and 8900 Å filter, very likely due to the influence in the flow

pattern of material coming from the SEBD site. The images in June show that the dark arm of the disturbance has encircled the planet almost totally, although there are still some unaffected longitudes (see Fig. 5).

The cylindrical maps in Fig. 6 and 7 visually summarize much of the previous comments and clearly show the evolution of the disturbance as seen in the red continuum and deep methane band filters. Due to the strong methane absorption at this wavelength, photons do not reach levels deeper than 300 mbar, so this map gives the appearance of the planet at higher atmospheric levels than continuum wavelengths do. The white spots of the disturbance are very bright in the strong methane band at 8900 Å, suggesting a higher effective cloud top in these regions than in the adjacent undisturbed regions. A complete limb-to-limb tracking of the disturbance was made during the mid-April observations in the 6190-9500 Å range, which will
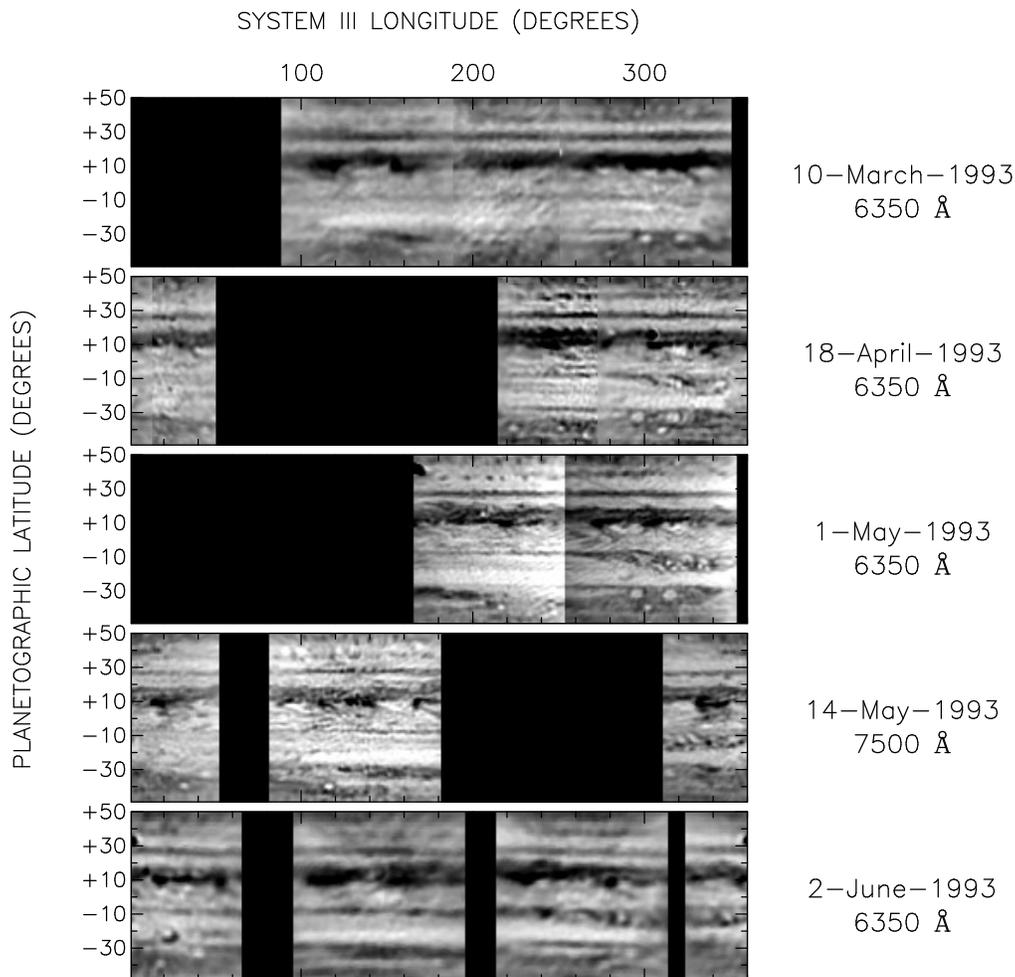
Fig. 6. Cylindrical maps at red continuum wavelengths. These maps were assembled from individual images acquired at different times and were corrected for limb darkening using a Minnaert law with a limb darkening coefficient of 1.

enable us to make an analysis of the limb darkening of the white spots and to infer the particle physical properties and size distribution compared to their surroundings.

During these stages of the disturbance, the geometrically normalized contrasts between the brightest spots and the NTrZ in the 6190-9500 Å range are close to 1 except at 8920 Å, in which the spots are 35% brighter than the NTRZ. Interestingly, these ratios are similar to that found for the GRS.

4. Activity in other Jovian regions

Not only has the SEB experienced a revival, but in addition, the South Temperate Belt (located near 30°S planetographic), that was absent for several years, was being revived in various dark sectors, as can be seen in Fig. 1. This figure shows a dark sector starting at the South Temperate Ovals ovals BC and DE in the image in March, 1993, which was not present in the image obtained during the previous apparition. In the northern hemisphere, the North North Temperate Belt (NNTB), located near 38°N planetographic, was also being revived as seen in Fig. 8. At some longitudes, NNTBs jetstream spots were seen, as shown in Fig. 6 and 7. These spots were also seen during the Voyager 2 encounter with Jupiter (Beebe et al., 1989).

The North Equatorial Belt (NEB) showed a double component with some sites of active convection (see Fig. 6), in which a chain of bright spots to the west of the eruption site is seen, and an oval in the interface of the NEB and NTrZ. This activity is rather typical of this region (Beebe et al., 1989). The North Temperate Belt was very uniform and did not show any morphological changes with respect to the previous apparition.

The South Tropical Zone showed the presence of various remarkable features. There were two spots at the same latitude as the GRS and showing the same photometric properties. The bigger one was at λ_{III}=288° on May 1st, and the smaller one was at λ_{III}=159° on May 14th (their dimensions were 7500 and 4500 km in diameter, respectively). These spots are bright in the 8900 Å methane band images (see Fig. 7). Our observations allowed to track the mean motion of the larger one, being of -0.44°day^{-1}, slightly greater than the mean speed of the GRS, estimated to be -0.34°day^{-1} in that period, significantly higher than its mean speed of -0.25°day^{-1} . These spots are the only features detected so far in the Southern hemisphere that are dark in the blue and very bright in methane. Similar features (the so-called Little Red Spots) are seen frequently in the NTrZ (Beebe and Hockey, 1986). The larger one in the STRZ was there at least since the last apparition and its flow pattern is also
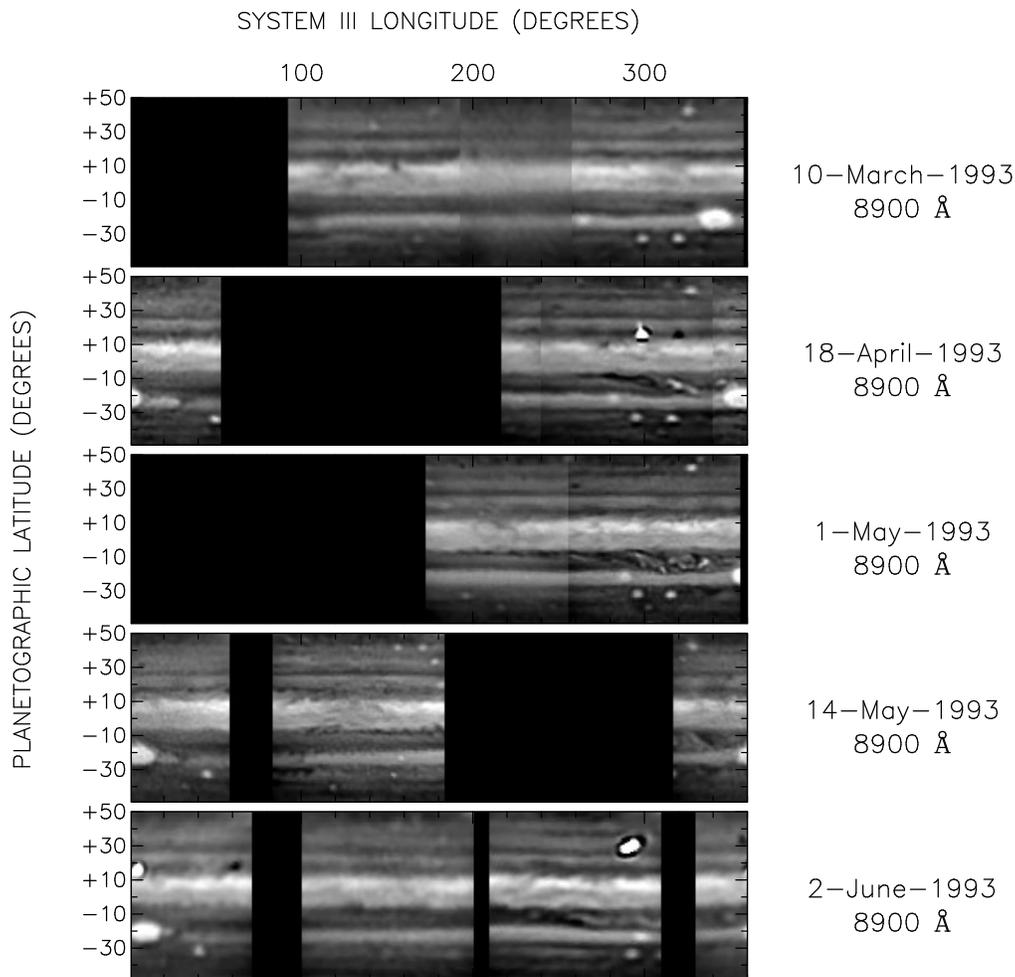
Fig. 7. Cylindrical maps at 8900 Åwavelength (strong methane band). These maps were assembled from individual images acquired at different times and were corrected for limb darkening using a Minnaert law with a limb darkening coefficient of 1.2. The saturated spots at System III longitudes near 300° in the map of April 18, and near 290° in the map of June 2 correspond to Galilean satellites.

anticyclonic. The geometrically normalized reflectivity of these spots compared to the NTRZ reflectivity in the wavelength range 0.37-0.95 micrometer is shown in Fig. 9. There were also some streaks resembling South Tropical Zone disturbances at various longitudes as seen in the cylindrical maps of Fig. 6 and 7. The most conspicuous ones are at λ_{III}=31 and 100° on May 14th. The first one is virtually stationary with System III, although it becomes accelerated, moving at a mean speed of $0.15°\mathrm{day}^{-1}$ from May 14th to June 2nd, likely as a result of its proximity to the GRS.

5. Location of the SEBD sources

The most important result regarding the location of the SEB disturbance is that it confirms the predicted position by the Reese's theory. For all the observed major SEB disturbances (from 1919 to 1971), Reese showed that three possible sources were well fitted to three parallel straight lines in a time versus System III longitude graphical representation. The source of the 1993 SEB revival confirms this result for the locus B. The site of the disturbance as predicted by Reese is just 7° apart from the actual place. In Fig. 10 we have plotted the previous major distur-

bances in the IAU currently used System III longitudes (Davies et al., 1983) associated to the locus B including the site of the 1993 SEB outburst. The result in the fitting process reveals that the residual error in the position is just 0.2°, much less than the 7° error using the Reese's formulae directly. This fact stresses the deep interior origin of this phenomenon. As mentioned previously, the apparition of the dark column was preceded by a dark streak north preceding the GRS. In fact, as revealed from our published narrow-band photometry during February 1992 (Moreno et al., 1993), this streak was already present there and the disturbance occurred exactly when the streak reached the predicted position of Reese's locus B. Obviously, these results cannot be attributed to a simple coincidence. Thus, for the first time, we report on the existence of a predictive feature preceding a major SEB revival. The resulting speed of the source B with respect to System III is $0.010\pm0.001°\mathrm{day}^{-1}$. Performing the same reasoning with respect to source A, including the major revivals in 1919, 1928, 1971 and 1975 (which showed a major eruption in locus A, followed by minor outbreaks), we obtained the same result, i.e., locus A is rotating exactly at the same speed as locus B with respect to the actual System III.
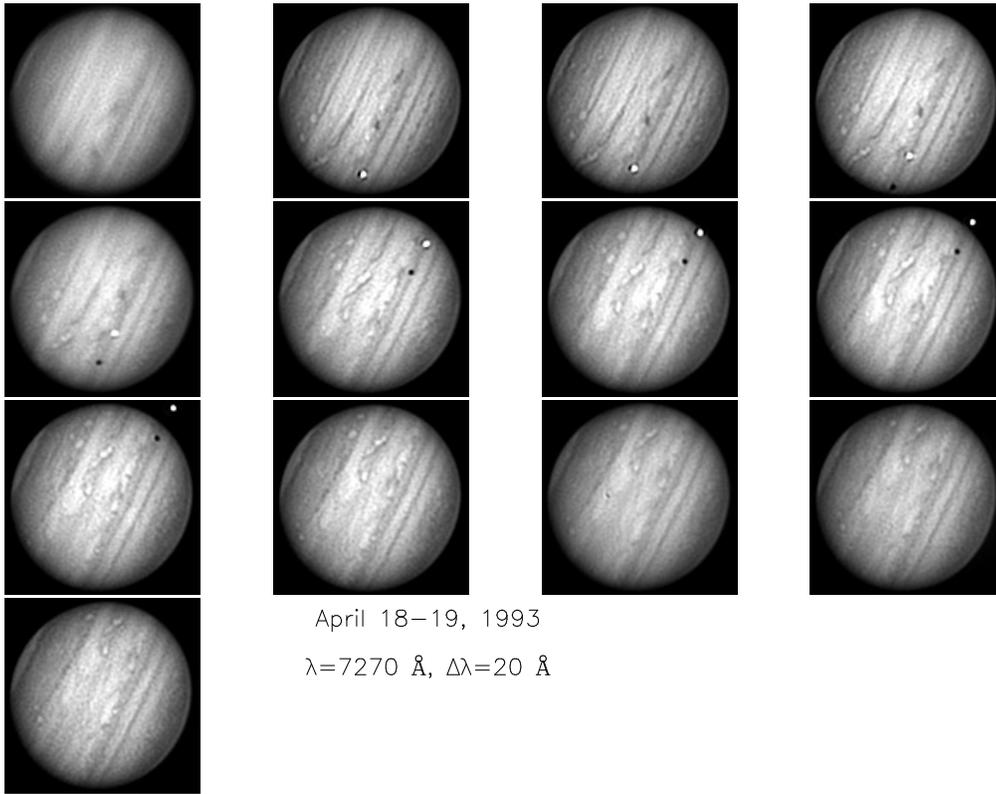
April 18−19, 1993

λ=7270 Å, Δλ=20 Å

Fig. 8. Temporal sequence of images acquired in the 7250 Å moderate absorption methane band showing the SEB disturbance moving from limb to limb and the revived North North Temperate Belt.

6. Characterization of the Jovian limb darkening as a function of latitude and wavelength

The acquisition of the large data set described above enabled us to characterize the different Jovian regions at the time of the observations from their limb darkening properties. The linear limb-darkening coefficients were obtained by fitting the experimental limb-to-limb curves to the Minnaert law at latitudes ranging from -65° to 65° planetographic at 5° step, and at the wavelengths shown in Table 1. This characterization of the different atmospheric regions has the main advantage of being independent of the absolute calibration in I/F. Given the large amount of wavelengths investigated, this determination could also be used as a reference in in future measurements.

The limb darkening coefficients as a function of wavelength and latitude were obtained from several images, and the result of the average of these determinations is shown in Fig. 11. To avoid crowding, the results concerning the images at 6190 and 7250 Å were not drawn in the graph. The error in these determinations was always less than 5% in the limb darkening coefficient.

There is a general trend in the variation of the coefficient with wavelength in the continuum: the coefficient increases with wavelength from the ultraviolet to the near-infrared, at all the Jovian latitudes. In the deep absorption methane band at 8900 Å, the coefficient is always larger than in the continuum wavelengths, a consequence of the existence of an absorbing gas above the effective cloud top, except for latitudes poleward of

+45° and -55°, in which the coefficient decreases dramatically. This is undoubtly due to the presence of the polar hazes high in the atmosphere, that account also for the high reflectivity observed at the poles. The south polar haze also influences the behaviour of the limb darkening at 3700 Å poleward of -50°. At equatorial latitudes, there is a remarkable sharp minimum which is seen at latitudes 10° to 15°, which corresponds to the position of the North Equatorial Belt. This minimum is followed by a local maximum in the coefficient at 20°, corresponding to the NTrZ (except for the curves corresponding to 3700 and 8900 Å).

For the sake of comparison, we also measured the limb darkening coefficient at one of the brightest features of the SEBD seen in the images acquired on April 18-19th (see Fig. 8). The spot is that located at λ_{III}=318° at the SEB latitude in the cylindrical map of April 18, 1993 (see Fig. 7). The resulting coefficients did not show any significative difference with respect to the SEB region in the 8900 Å region, but they do show values of the coefficient that decrease slightly with wavelength in the continuum filters at 6350, 7500, and 9500 Å (see Fig. 12), a behaviour which is opposite to the general behaviour found at all the Jovian latitudes, and that may be indicative of a different particle size distribution and/or particle loading in different atmospheric layers that would be implied by the vigorous dynamics governing the spots associated to the SEBD event.
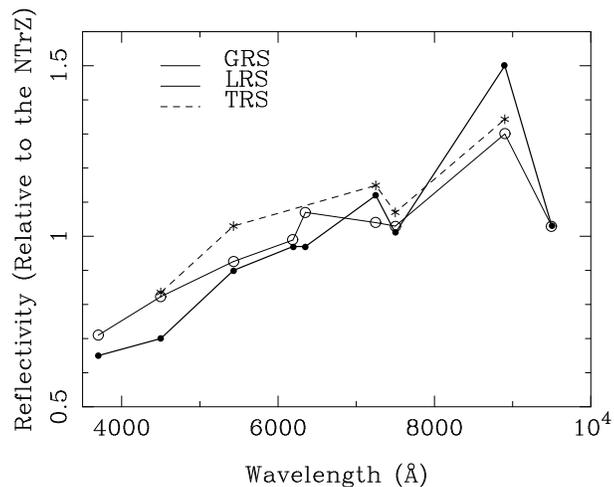
Fig. 9. The photometric spectral variations of little red spots in the South Tropical Zone and the GRS. The curve labeled "GRS" corresponds to the geometrically normalized reflectivity of the Great Red Spot divided by that of the North Tropical Zone (NTrZ). The curve labeled "LRS" corresponds to a little red spot which can be clearly seen in the cylindrical map of Fig. 7 in the panel corresponding to May 1, 1993 at λ_{III}=288° and at the same latitude where the GRS is located. It is also clearly seen at longitudes nearby in all the maps except on May 14, where no data at those longitudes were acquired. The curve labeled "TRS" corresponds to a tiny red spot which is seen at λ_{III}=159° and at the latitude of the GRS in the panel corresponding to May 14, 1993 (see Fig. 7).
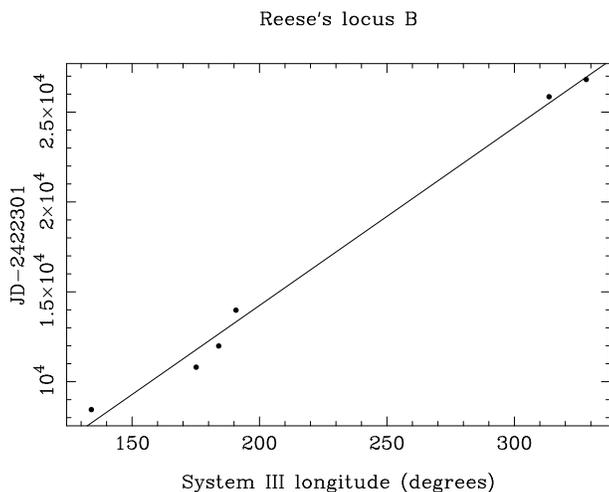

Fig. 10. The position of the SEB major eruptions associated to the Reese's locus B versus time. The source B moves at a speed of 0.010±0.001°day^{-1} with respect to System III longitude.
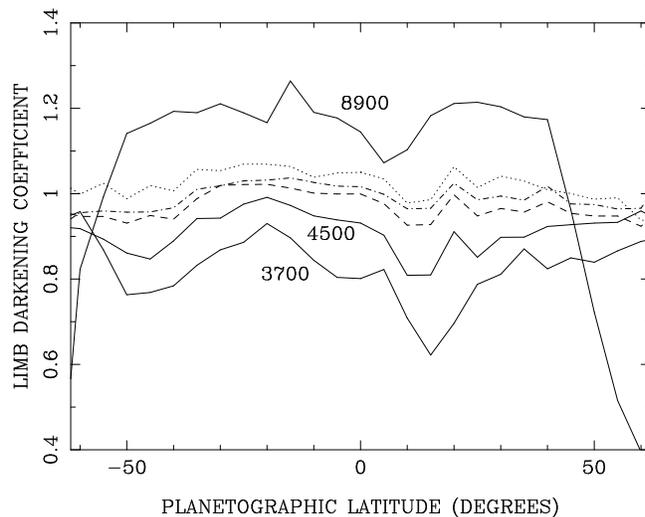
Fig. 11. The Minnaert limb darkening coefficient as a function of latitude for various wavelengths. The solid lines correspond to 3700 Å, 4500 Å, and 8900 Å, as indicated. The dashed line correspond to the wavelength of 6350 Å, the dot-dashed line to 7500 Å, and the dotted line to 9500 Å. Note the increase in the limb darkening coefficient at every latitude on Jupiter as the wavelength increases for all the continuum wavelengths.
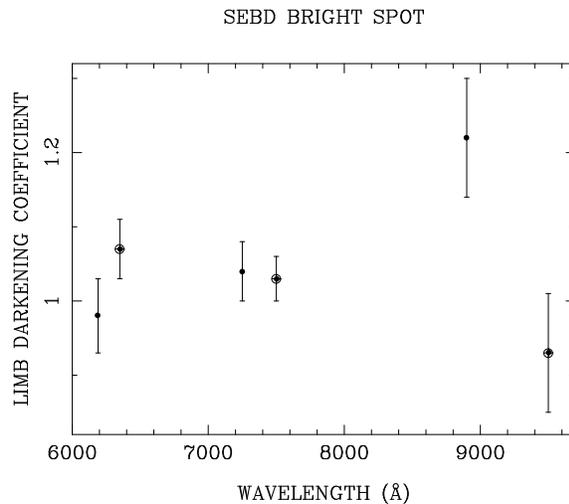

Fig. 12. The limb darkening coefficient as a function of wavelength for the brightest spot associated to the SEBD as a function of wavelength. Note in this case a decrease in the magnitude of the coefficient as a function of wavelength in the continuum (6350, 7500, and 9500 Å, encircled solid dots).

References

Beebe, R.F., and Hockey, T.A., 1986, Icarus 67, 96

Beebe, R.F., Orton, G.S., and West, R.A., 1989, In *Time-Variable Phenomena in the Jovian System*, eds. M.J. Belton, R.A. West and J. Rahe. NASA SP-494, Washington DC.

Chanover, N.J., Beebe, R.F., and Kuehn, D.M., 1993, Bull. Amer. Astron. Soc. 25, 1037

Chapman, C.R. and Reese, E.J., 1968, Icarus 9, 329

Davies, M.E., Abalakin, V.K., Lieske, J.H. et al., 1983, Celestial Mechanics, 29, 309

Molina, A., Moreno, F., and Ortiz, J.L., 1993, Bull. Amer. Astron. Soc., 25, 1037

Molina, R., Ripley, B.D., Molina, A. et al., 1992, Astron. J. 104, 1662

Moreno, F., 1993, Bull. Amer. Astron. Soc., 25, 1041

Moreno, F., Molina, A., and Ortiz, J,L., 1993, J. Geophys. Res., 98, 18837

Orton, G., Friedson, J., Yanamandra-Fisher, P. et al., 1993, Bull. Amer. Astron. Soc., 25, 1035

Peek, B.M., 1958, *The Planet Jupiter*. Faber and Faber, London

Reese, E.J., 1972, Icarus, 17, 57

Rogers, J., 1993, J. Br. Astron. Assoc., 103, 157

Sanchez-Lavega, A., Gomez, J.M., Miyazaki, I. et al., 1993, Bull. Amer. Astron. Soc. 25, 1037

Sanchez-Lavega, A., Gomez, J.M., Lecacheux, J. et al., 1996, Icarus, 121, 18